

Perspective

Proton conductors for heavy-duty vehicle fuel cells

Craig S. Gittleman,¹ Hongfei Jia,² Emory S. De Castro,³ Calum R.I. Chisholm,⁴ and Yu Seung Kim^{5,*}

SUMMARY

Fuel cells utilize the chemical energy of liquid or gaseous fuels to generate electricity. As fuel cells extend their territory to include heavy-duty vehicles, new demands for proton conductors, a critical component of fuel cells, have emerged. A near-term need is ensuring the chemical and mechanical stability of proton exchange membranes to enable long lifetime vehicles. In the mid-term, achieving stable conductivity of proton conductors under hot ($>100^{\circ}\text{C}$) and dynamic fuel cell operating conditions is desirable. In the long term, targeting high thermal stability and tolerance to water enables the utilization of high energy density liquid fuels that will increase pay-load space for heavy-duty vehicles. This article presents our perspective on these near-, mid-, and long-term targets for proton conductors of heavy-duty fuel cells.

INTRODUCTION

The utilization and storage of hydrogen produced from renewable, nuclear, or fossil fuels with carbon capture can help decarbonize the U.S. and global economies and avoid the worst effects of climate change. In the mid-1970s, the United States Department of Energy (US DOE) touted the promise of hydrogen as a clean transportation fuel and consequently started proton exchange membrane fuel cell (PEMFC) research and development programs. The Energy Policy Act Title VIII on hydrogen in 2005 further promoted innovative hydrogen and fuel cell technologies. Recently, the US DOE Energy Efficiency Renewable Energy (EERE) Hydrogen and Fuel Cell Technologies Office (HFTO) initiated the H2@Scale concept for wide-scale hydrogen production and utilization.¹ HFTO also announced the Million Mile Fuel Cell Truck Consortium (M2FCT) that supports early-stage R&D for widespread commercialization of heavy-duty vehicle (HDV) fuel cells. The 2025 target for M2FCT is to achieve $2.5\text{ kW g}^{-1}\text{ PGM}$ power (1.07 A cm^{-2} current density) at 0.7 V after a 30,000 h-equivalent of accelerated durability testing. In addition to hydrogen, interest in the utilization of low carbon or carbon neutral liquid fuels is growing, as liquid fuels have a higher energy density and require significantly less infrastructure investment.² The US DOE EERE HFTO and Advanced Research Projects Agency-Energy (ARPA-E) have supported fuel cell programs to implement various liquid fuels, including methanol, dimethyl ether, hydrazine, and ammonia. A part of the motivation for developing liquid fuels is the fact that large-scale distribution of hydrogen typically involves compression and/or liquification at -253°C , and hence, storage and distribution costs of hydrogen account for as much as 50% of the energy delivered. Aside from production by reforming processes, high energy density liquid fuels can also be made through greener pathways. One employs hydrogen generated from water electrolysis via renewable electricity (e.g., wind or solar power), which is combined with CO_2 from either an emitter, such as a fossil fuel power plant, or a carbon capture and utilization process.³ A second pathway involves the conversion of plant-based

Context & scale

Fuel cells are an attractive technology to power zero-emission vehicles. Compared with battery-powered vehicles, fuel cells offer fast fueling and adequate fuel storage for long-range applications. Heavy-duty fuel cell vehicles have strenuous requirements with the most challenging target being the development of fuel cells with the durability to return capital investment over a longer lifetime. Fuel cell operation under hot and dry conditions enables simpler, low-cost fuel cell systems through better heat and water management. Utilizing high energy density liquid fuels can also increase pay-load space and eliminate the need for an expensive hydrogen infrastructure. Advanced proton conductors that can resolve these issues associated with heavy-duty fuel cell applications are needed. Here, we present the progress and promising options in meeting near-, mid-, and long-term targets with respect to performance, durability, and technical readiness to stimulate research on proton conductors for heavy-duty fuel cell vehicles.

bio feed stocks into liquid hydrocarbon fuels.⁴ Through either of these two pathways, one can create and use hydrogen carriers that reduce emissions. While high energy density liquid fuels are also used in internal combustion engines (ICEs),⁵ the high combustion temperatures of ICEs typically lead to other unwanted pollutants such as NO_x and SO_x. Because fuel cells do not rely on combustion, they avoid the generation of these pollutants.

Fuel cells convert chemical potential energy into electrical energy. At the anode, a catalyst activates the hydrogen to undergo an oxidation reaction that generates protons and electrons. The generated protons are transported through a proton-conducting membrane to react with oxygen and electrons to produce water at the cathode (Figure 1A). The industrial-standard proton-conducting materials are perfluorosulfonic acids (PFSA), while other material options include functionalized hydrocarbon polymers, metal-organic frameworks, metal phosphates, and their composites with acids and ionic liquids. As fuel cells gain interest in HDV primary powertrain applications, more stringent requirements for proton conductors have been identified (Figure 1B). Improving electrochemical and mechanical stability of low-temperature proton exchange membrane fuel cells (LT-PEMFCs) is the most pressing priority in the near term. According to the US DOE's multi-year research, development, and demonstration plan, a 30,000 h lifetime, approximately four times that of the light-duty vehicles (LDV target: 8,000 h), is required for HDV applications.⁶

In the mid-term, simplification of fuel cell systems through better heat and water management is imperative. Such a requirement is closely related to the automotive heat rejection constraint.⁷ In the current LT-PEMFCs, the temperature difference between the fuel cell temperature (60°C–80°C) and the ambient temperature (up to 50°C in hot climates) is relatively small when compared with ICEs. This small temperature difference between the fuel cell and ambient temperatures poses a significant challenge for designing a small and lightweight cooling system. The current radiator for fuel cells is much larger, more complicated, and more expensive than that of ICEs. The low-temperature operation further causes a heat rejection constraint when operating the fuel cell at high current densities. To achieve higher power for HDV fuel cell applications, increasing the operating temperature to above 100°C is desirable. Hot and dry fuel cell operating conditions also provide the benefit of superior contaminant tolerance, which enhances the overall efficiency of reforming energy systems.⁸ As sulfonated proton conductors used in LT-PEMFCs have poor conductivity at low relative humidity (RH), it is critical to develop anhydrous proton conductors that enable high operating temperature.

In the long-term, fuel cells that utilize high energy density liquid-fuel offer an attractive option due to the difficulties of transporting hydrogen over long distances and the low volumetric energy density of hydrogen. Since the fuel-reforming temperature of a broad range of hydrocarbons or carbon-free fuels occurs above 200°C, a further increase in the fuel cell operating temperature is desirable. Additionally, these fuel cells should also have high tolerance to water and other fuel processing by-products, which are problematic for polybenzimidazole/phosphoric acid membranes. Therefore, the development of advanced high-temperature proton conductors is essential for liquid-fueled fuel cells. A further increase in fuel cell operating temperatures to above 300°C, which is the preferred temperature range for liquid fuels, can be achieved by using proton-conducting ceramics. However, the fast and deep load changes of automotive fuel are extremely stressful at such high operating temperatures. Thus, the fuel cells that operate at >300°C normally require

¹Global Fuel Cell Business, General Motors, Pontiac, MI 48340, USA

²Material Research Department, Toyota Research Institute of North America, Ann Arbor, MI 48105, USA

³Advent Technologies, Charlestown, MA 02129-1662, USA

⁴SAFCCell, Pasadena, CA 91106, USA

⁵MPA-11: materials synthesis and integrated devices, Los Alamos National Laboratory, Los Alamos, NM 87545, USA

*Correspondence: yskim@lanl.gov

<https://doi.org/10.1016/j.joule.2021.05.016>

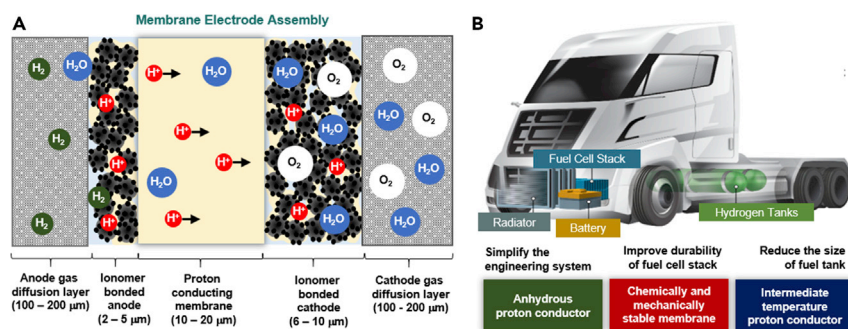


Figure 1. Proton conductors in fuel cells

(A) Schematic illustration of the cross-section of membrane electrode assembly in a fuel cell.
(B) Benefits of advanced proton conductors for HDV fuel cells.

battery hybridization. In addition, the benefits of faster fuel cell kinetics and the improved heat rejection at high operating temperatures are largely diminished by accelerated corrosion and the limited material choices for cell components.

In this perspective, we present the progress of next-generation proton conductors in meeting these requirements from the original equipment manufacturer's view. Specifically, we focus on the current advancement of proton conductors in achieving high durability and better heat and water management by operating fuel cells at higher operating temperatures (80°C–300°C) and utilizing high energy density liquid fuels.

Near-term challenges: Chemically and mechanically stable membranes for LT-PEMFCs

Early fuel cell developments in 1995 reported 60,000 h of durability during continuous fuel cell operation at 43°C–82°C using a thick PFSA membrane (Nafion 120, 250 μm thick).⁹ However, the stability of PFSA membranes became an issue as thinner membranes were employed for automotive fuel cells to increase power density. During the 2000s, the durability of fuel cells for bus applications was evaluated by Ballard Power Systems. Their P5 stacks (2002) with 50 μm-thick PFSA membranes lasted approximately 3,000 h, while an HD6 module (2007) using a 25 μm-thick PFSA membrane ran for 6,842 h.¹⁰ Since early 2010s, various accelerated stress tests (ASTs) have been developed to evaluate the stability of membranes within a shorter time frame.¹¹ The ASTs were based on the fact that membrane degradation during simultaneous chemical and mechanical stressors occurs much faster than when exposed to individual stressors.^{12,13} Moreover, it has been found that a properly designed, combined chemical and mechanical AST replicates the degradation and failure modes of field operation.¹⁴ In a combined open-circuit voltage (OCV) and RH cycling AST protocol at 90°C, the PFSA membranes used for P5 and HD6 modules failed after approximately 100 and 200 h, respectively, with observed failure modes of cracking in both membranes as well as local thinning. A mechanically and chemically stabilized PFSA membrane (Nafion XL, 27.5 μm-thick) developed in 2010 failed after ~675 h in this combined AST protocol. The thinning rate of the Nafion XL membrane was ~3 times lower than the membrane used for the Ballard HD6 module. The projected lifetime of a fuel cell using Nafion XL was ~20,000 h, which is still lower than the DOE 2025 HDV target (30,000 h). Even thinner membranes (10–15 μm thick) are currently being used for LDV applications. A 12 μm-thick membrane with a mechanical support and a chemical stabilizer used as an M2FCT benchmark passed the 8,000 h LDV equivalent target in an AST.¹⁵ Compared with LDV applications,

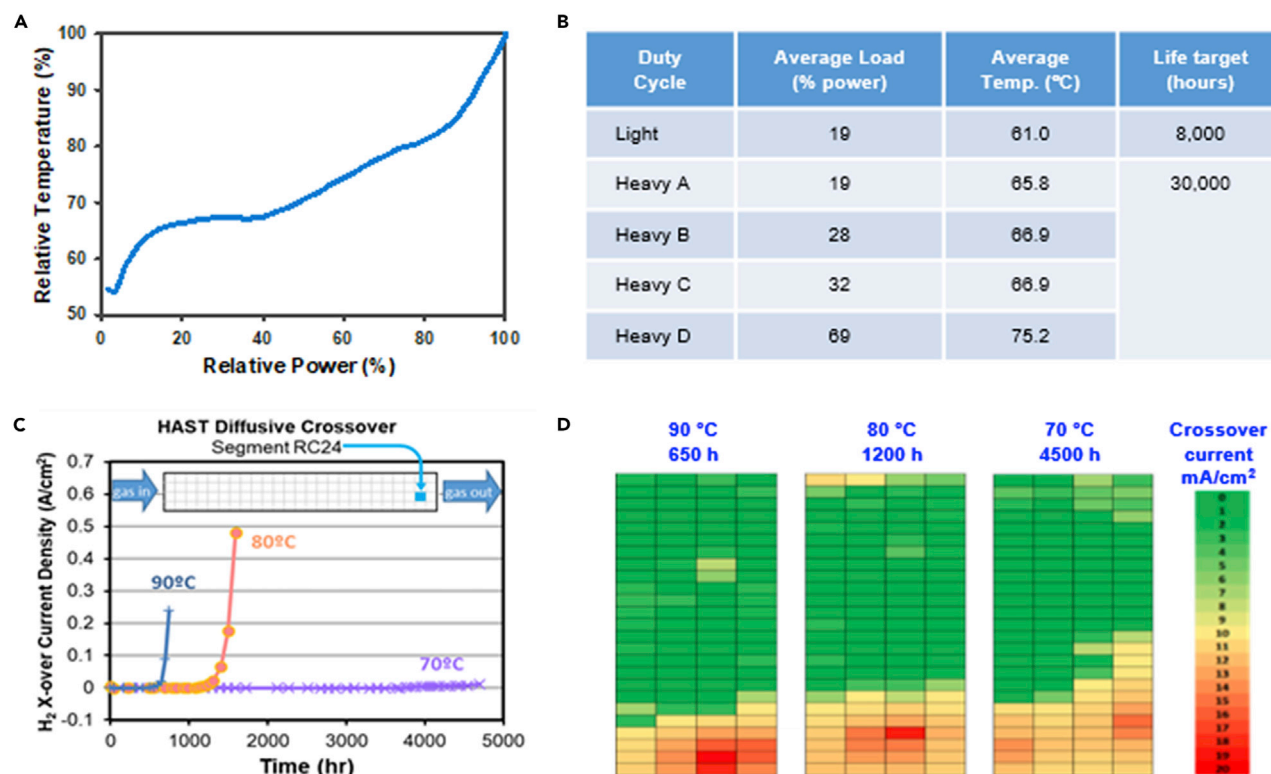


Figure 2. Impact of operating temperature on fuel cell durability

(A) Stack relative coolant outlet temperature as a function of relative percentage of maximum fuel cell power.

(B) Average operating temperatures for a common fuel cell system operating under various LDV and HDV drive cycles.

(C) Local H₂ diffusive crossover as a function of time for the combined AST tests at 70°C, 80°C, and 90°C.

(D) H₂ diffusive crossover maps toward the end of the combined AST tests at 70°C, 80°C, and 90°C. Crossover values are in mA/cm². The data were reproduced from Lai et al.¹⁶

membranes for HDV applications require greater stability at higher operating temperatures because HDV fuel cell systems run at a higher average percentage of peak load. The stack temperature relative to its peak operating temperature for a state-of-the-art fuel cell system as a function of its power relative to its maximum load is shown in Figure 2A, which indicates that a stack runs hotter at a higher relative power. Figure 2B shows the relative load and average stack temperature for typical light-duty and several heavy-duty drive cycles for a fuel cell system with the load-temperature curve shown in Figure 2A. The average operating temperature of HDV fuel cells could be 5°C–15°C higher than an LDV system depending on the duty cycle even if the peak operating temperature for both systems is the same. Thus, while the target lifetimes for HDV applications are higher than LDVs, the expected higher operating temperatures makes meeting these targets even more challenging.

Operating temperature is one of the most significant factors that impact the durability of LT-PEMFCs. Figure 2C shows the local hydrogen crossover current density change of PFSA-based fuel cells during the General Motors' (GM) combined stressor highly accelerated stress test (HAST) as a function of temperature.¹⁶ A cell operated at 70°C showed initial signs of hydrogen crossover at 4,700 h while a cell operated at 80°C failed to run after 1,600 h. The lifetime of the cell run at 90°C is less than 750 h. This HAST result is consistent with the durability tests of an 80 kW fuel cell system in which the cell lifetime decreases by about half with each 10°C temperature increase.

The degradation location for the HAST cells can be seen in the segmented hydrogen diffusive crossover maps measured toward the end of the test in Figure 2D, where the co-flow H₂ and air gas inlets are at the top of the maps. The *in situ* diagnostic analyses indicate that the degradation progression of these cells is identical at the three temperatures with crossover developing toward the gas outlets. The postmortem analyses suggested that membrane degradation is manifested as a thinning that occurs where the synergistic effect between mechanical and chemical stress is highest. Such a thinning is indicative that chemical degradation is the primary failure mode.

The chemical degradation of sulfonated membranes is mainly attributed to reactive free radical species, such as OH•, which are generated *in situ* through electrochemical pathways during fuel cell operation.¹⁷ The most common and efficient way to improve the chemical stability of PFSA is to use radical scavengers. Cerium, as either an ion or an oxide,¹⁸ and heteropolyacids (HPAs),¹⁹ are radical scavengers that have proven to be effective. A small amount of Ce incorporated into PFSA effectively quenches the reactive free radical species faster than they react with the polymer with little impact on membrane performance and mechanical durability.¹² A postmortem analysis of the membrane electrode assemblies (MEAs) from the HAST results shown in Figure 2C, revealed Ce, which was used as a stabilizer, was depleted from the cell outlet region. This suggests that migration of the mobile Ce cations contributed to the relatively early failure in that region.¹⁶ Other studies have also shown that Ce migration can lead to early membrane failure as stabilization against reactive free radical species is reduced in Ce-depleted regions.^{20,21}

As Ce ions are mobile under fuel cell operating conditions, concepts to immobilize the radical scavengers are being developed. One approach to immobilize Ce ions is to use cerium oxide^{22,23} or mixed metal oxides such as cerium zirconium oxide (CeZr_xO_y) nanoparticles or nanofibers.²⁴ Baker et al. have shown that the polymetallic oxides exhibit better peroxide scavenging activity and dissolution resistance than undoped ceria.²⁵ Researchers at GM have demonstrated that an MEA using a CeZrO₄-incorporated PFSA membrane showed a significantly reduced fluoride release rate (FRR) during an OCV test as compared with a non-stabilized membrane. The FRR of the MEA using a CeZrO₄-incorporated PFSA membrane approached the FRR level when using the Ce nitrate salt (Figure 3A). With further optimization, we hope that CeZr_xO_y nanoparticles will match the stabilization effect of the Ce salt. They also showed negligible local Ce redistribution within the membrane after 85 h at 1.0 A cm⁻², 80°C, and 100% RH (Figure 3B).¹⁵ HPAs, such as 11-silicotungstic acid, have been used to enhance proton conductivity under dry conditions while also improving chemical stability. However, the incorporation of sufficient HPA content into membranes to meet conductivity targets makes the membranes brittle. A new concept uses a PFSA for the primary proton-conducting medium combined with a relatively small amount of HPA for chemical stabilization, thus getting around the brittleness problem caused by high HPA content. To immobilize the HPA, sulfonyl fluoride PFSA precursors with reactive anchor points were synthesized to tether HPA particles to the polymer through covalent bonds (Figure 3C).¹⁵

Enhancing the mechanical stability of thin PFSA membranes is achieved mainly by incorporating structural reinforcements²⁶ and utilizing high molecular weight ionomers.²⁷ The most common and effective type of reinforcement, or support layer, is an expanded poly [tetrafluoroethylene] (ePTFE). The ePTFE's properties can be tailored to maximize durability by reducing in-plane membrane swelling while

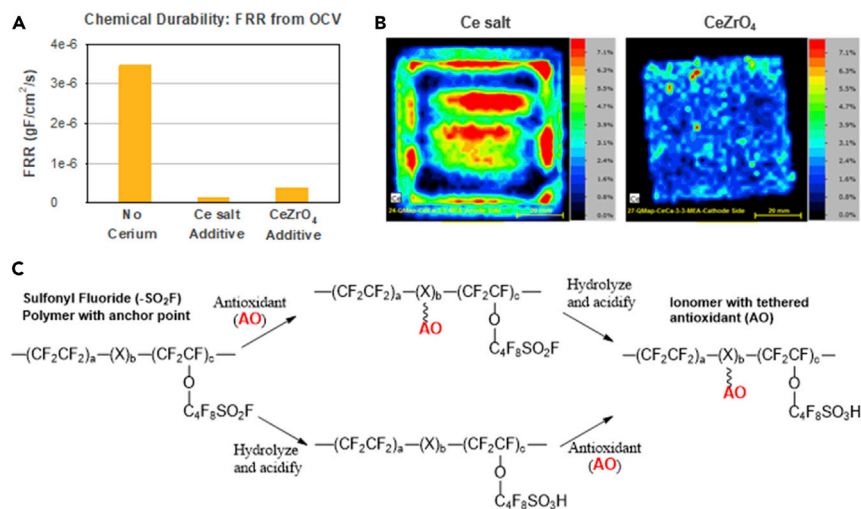


Figure 3. Approach to improve electrochemical stability of PEM

(A) Fluoride release rate (FRR) during 200 h-OCV tests at 95°C and 25% RH of PFSA membranes with and without Ce stabilizers.

(B) Ce X-ray fluorescence map of Ce salt-stabilized PFSA membrane and Ce_xZr_yO₄ nanofiber stabilized PFSA membrane after 85 h at 1.0 A/cm², 80°C, and 100% RH in a 50 cm² serpentine flow field cell.

(C) Reaction scheme of immobilizing HPA into a PFSA polymer using a sulfonyl fluoride polymer precursor. Reproduced from Ramaswamy¹⁵ with permission.

simultaneously minimizing proton transport losses.²⁸ Another approach to improving the stability of membranes is to use sulfonated polyaromatics.²⁹ Compared with the industrial-standard PFSA membranes, sulfonated polyaromatic membranes have low reactant gas permeability that improves not only fuel cell efficiency by reducing the hydrogen crossover current but also the chemical stability of membranes. It is known that the crossover oxygen from the cathode forms hydrogen peroxide at the anode potentials.³⁰ The hydrogen peroxide is decomposed in the presence of impurity cations to generate oxygen radicals and causes membrane degradation. Sulfonated aromatic membranes also have higher mechanical strength and modulus, which makes it possible to cast thin film without reinforcement. However, the practical uses of sulfonated polyaromatic membranes are limited by their strong dependence on RH for proton conductivity, which requires a high level of humidification. Low conductivity at low RH can be improved by increasing the concentration of the sulfonic acid groups.³¹ However, the incorporation of a high concentration of sulfonic acid groups in the polymers makes the membranes brittle in a dry state and causes excessive swelling in a wet state.^{32,33} The brittleness of highly sulfonated polyaromatics in a dry state makes it difficult to handle and subject to cracking, while excessive swelling in the wet state increases mechanical stress. This phenomena is particularly troubling at the edge of the MEA active area and regions where the hydration level of the membrane significantly changes during operation.³⁴ Additionally, the high modulus of sulfonated aromatic membranes, combined with their relatively high swelling, leads to exorbitant stress during humidity cycling, which in turn leads to poor mechanical durability. As a result, most sulfonated polyaromatic membranes suffer premature failures and do not survive during wet-dry cycling ASTs.³⁵ More research efforts on improving the mechanical stability of sulfonated polyaromatic membranes under wet-dry cycling conditions are necessary. Intrinsic susceptibility to radical-induced chain degradation of sulfonated polyaromatics also needs further study. This issue cannot be addressed by the

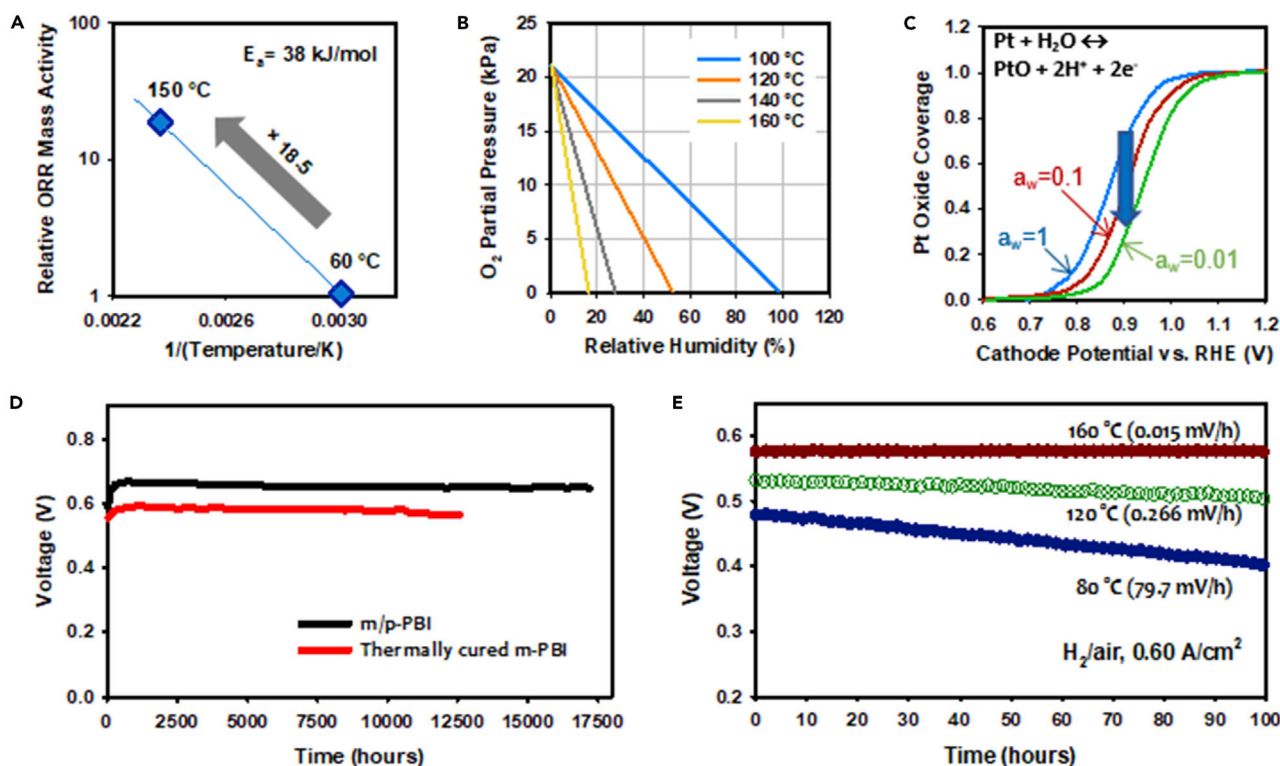


Figure 4. Effect of temperature on catalyst activity and durability of PA-PBI-based fuel cells

(A) Effect of catalytic activity of Pt on oxygen reduction reaction.

(B) Dependence of O_2 partial pressure on temperatures at 100 kPa_{abs}. Assume there is no back pressure.

(C) Pt oxide coverage as a function of water activity.³⁷

(D) PA-PBI HT-PEMFC durability at 160°C.⁴⁰ Membrane: meta/para-PBI (m/p-PBI (7:1)) or thermally cured meta-PBI (m-PBI).

(E) Impact of operating temperature of durability of HT-PEMFC under anhydrous conditions. The H_2 /air performance was measured at 0.6 A cm⁻² under anhydrous conditions.

conventional stabilizers that work well with PFSA as the hydroxyl radical reacts faster with the aromatic ring than it does with Ce^{3+} .³⁶

Mid-term challenges: Acid retention in the presence of water for HT-PEMFCs

The primary benefit of operating fuel cells under hot and dry conditions for vehicular applications is the simplification of the fuel cell system due to smaller radiator size via better thermal management and humidifier elimination. These conditions may enhance catalytic activity, improve oxygen transfer via higher oxygen partial pressure by removing water in the MEA, and reduce Pt oxide formation in the absence of water (Figures 4A–4C).³⁷ The operation of sulfonated membrane-based fuel cells under hot and dry conditions is challenging^{38,39} because sulfonic acid groups require water for the necessary proton conduction. Moreover, reasonable durability of fuel cells using sulfonated membranes (>1,000 h) has not been demonstrated under these conditions. Phosphoric acid-doped membranes such as phosphoric acid-doped benzimidazoles (PA-PBIs) have high proton conductivity (~ 0.1 S cm⁻¹), and the PA-PBI-based fuel cells have exhibited stable operation for long times (e.g., >17,000 h at 160°C,⁴⁰ and >10,000 h at 180°C⁴¹) (Figure 4D).⁴² A key bottleneck of the automotive fuel cells employing PA-PBI membranes is the cell stability at low operating temperatures (<140°C). Figure 4E shows the cell voltage change of PEMFCs using a PA-PBI membrane at three different operating temperatures (160°C, 120°C, and 80°C). The fuel cell operating at 160°C was stable with a low

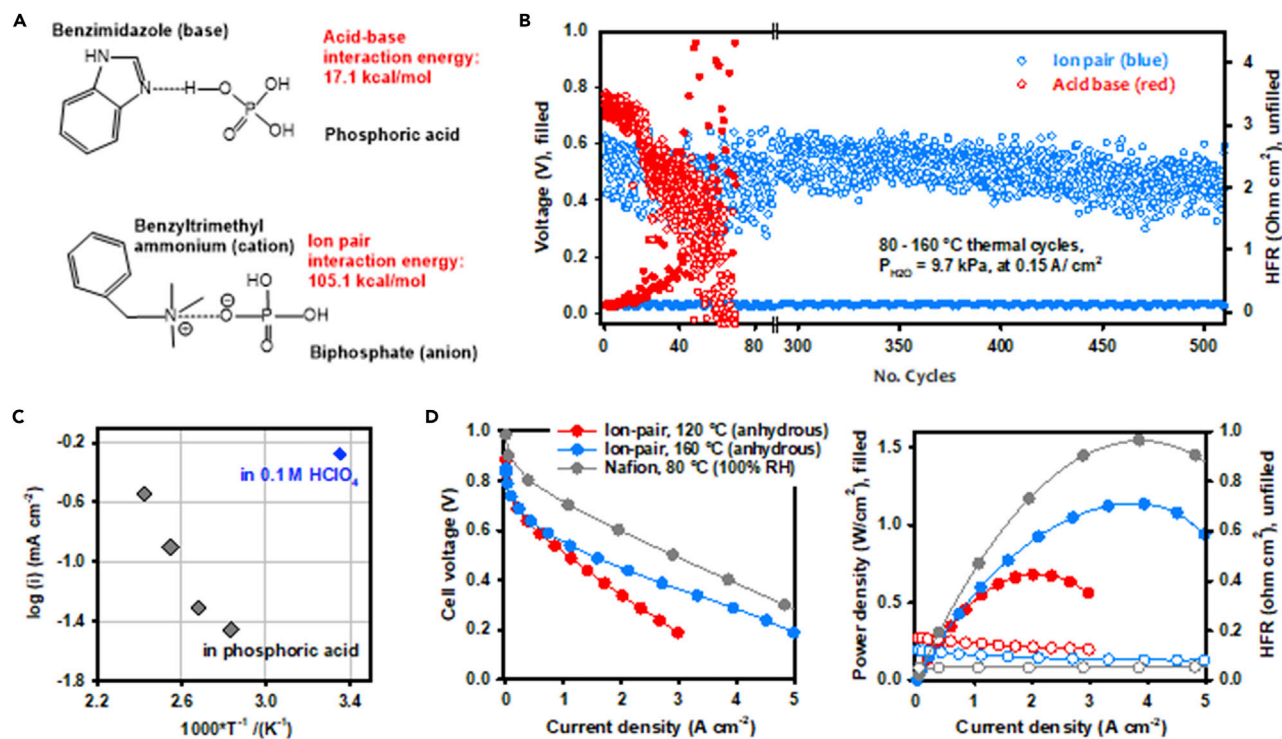


Figure 5. Approach to improve acid retention of HT-PEMFCs

(A) Interaction energy comparison between acid-base and ion-pair.⁴³

(B) Comparison of water tolerance between acid-base and ion-pair HT-PEMFC MEAs. HFR and voltage change of the MEAs during thermal cycles of 80°C–160°C at a constant water vapor pressure of 9.7 kPa. The cell was operated at 0.15 A cm⁻². Reproduced with permission.⁴¹ Copyright 2016, Springer Nature.

(C) The ORR current density of Pt catalyst in phosphoric acid and 0.1 M HClO₄. For Pt/C activity in phosphoric acid (80°C, 100°C, 120°C, and 140°C), the potentials of electrode were adjusted to 0.825, 0.810, 0.787, and 0.779 V versus RHE, respectively (0.2 V below the measured OCV). The Pt/C activity in 0.1 M HClO₄ at 25°C was measured at 0.9 V versus RHE.

(D) H₂/O₂ fuel cell performance at 120°C and 160°C under anhydrous conditions. Ion-pair MEA, PEM: PA-QAPOH (thickness: 40 μm), Anode catalyst: PtRu/C (0.5 mg_{Pt} cm⁻²), Cathode: Pt/C (0.6 mg_{Pt} cm⁻²). The fuel cell performance obtained the H₂/O₂ (500/500 sccm) under 147.1 kPa_{abs} backpressure without humidification. Nafion MEA, PEM: Nafion (thickness: 25 μm), Anode catalyst Pt/C (0.6 mg_{Pt} cm⁻²), Cathode: Pt/C (0.6 mg_{Pt} cm⁻²). The fuel cell performance obtained the H₂/O₂ (500/500 sccm) under 285 kPa_{abs} backpressure with 100% RH. Reproduced with permission.⁴⁹ Copyright 2021, Springer Nature.

voltage decay rate (0.015 mV h⁻¹). However, as the operating temperature decreased to 120°C and 80°C, the voltage decay rate increased to 0.266 and 79.7 mV h⁻¹, respectively. The performance loss at the low operating temperature is primarily related to the phosphoric acid loss in the presence of water. This limits the operation temperature of PA-PBI based on fuel cells to above 150°C and also requires a high-power battery system for fast fuel cell startup.

The phosphoric acid loss is related to the phosphoric acid equilibrium partition composition.⁴³ Because the interaction energy of phosphoric acid-benzimidazole is lower than that of phosphoric acid-benzimidazole-water, the phosphoric acid in the polymer is replaced with water and the acid content decreases upon hydration. Understanding such a mechanism provides a pathway to improving phosphoric acid retention by introducing stronger ion-pair interactions (Figure 5A). Instead of using basic functionality, as in PBI, cation functionality can increase the equilibrium composition of phosphoric acid, and thus, a higher water vapor pressure is required to exchange for the phosphoric acid in the polymer. Lee et al. first prepared an ion-pair membrane that coordinated biphosphate anions and quaternary

ammonium cations (PA-QAPOH).⁴⁴ The high phosphoric acid retention of the ion-pair membrane was confirmed in a temperature-cycling AST (80°C to 160°C) with a water partial vapor pressure of 9.7 kPa (Figure 5B). Note that the voltage of the PA-PBI MEA decreased from 0.78 to ~0 V within only 70 cycles. In contrast, the performance of the ion-pair MEA was stable over 500 thermal cycles, maintaining the initial performance throughout the AST. The high acid retention of ion-pair coordinated polymers enables stable operation at 80°C under high current generating conditions (~2 A cm⁻²).

One technical challenge of the ion-pair membrane-based fuel cells is their performance. It is known that phosphoric acids can poison the catalysts with chemisorbed dihydrogen phosphate (H₂PO₄⁻) and hydrogen phosphate (HPO₄²⁻) ions,^{45,46} as shown by the significantly lower oxygen reduction reaction (ORR) activity of Pt/C and Pt disk in phosphoric acid versus perchloric acid (Figure 5C). Low oxygen permeability⁴⁷ and electrode flooding⁴⁸ further lowers electrode performance. Phosphonated polymers that have lower acid content may improve the performance of ion-pair MEAs.⁴⁹ However, the performance of ion-pair MEAs in the kinetic region (>0.7 V) is still substantially lower than a Nafion-based LT-PEMFC (Figure 5D). Alloy catalysts that mediate the poisoning reaction, such as in the case of typical phosphoric acid fuel cells, may improve performance. Besides acid retention and fuel cell performance, startup capability at low temperatures (-30°C), development of high-temperature compatible, non-functional materials (seals, gaskets, adhesives), and high-temperature corrosion and creep-resistant materials require more attention to make the system suitable for HDV applications due to longer lifetime requirements compared with LDV applications. However, many of these challenges, if not all, can be resolved by improving system design and control, including sealing strategies to eliminate the needs of polymer seals, carefully programmed startup and shutdown procedures to minimize the exposure to liquid water and stress from material thermal expansion/contraction, and more efficient thermal management to reduce stack size. For example, operating HDVs at a rated power of over 100°C enables the exploitation of latent heat systems (phase change of liquid coolant), leading to a greater heat capacity than the sensible heat of any typical cooling fluid, which promotes smaller radiators and lower wind drag designs. The benefits of HT-PEMFCs can be further strengthened by choosing a range extender type of hybrid system, which uses a large battery pack to provide the main power for driving the motors. In this system configuration, the HT-PEMFC stack operates under the highly efficient steady-state condition to charge the batteries for extended driving distances. Such a hybrid platform not only helps overcome the inherent shortcoming of HT-PEMFC's slow startup but also takes advantage of the long lifetimes that have already been demonstrated under constant current operation.

Long-term challenges: High-temperature (>200°C) proton conductors for liquid-fueled fuel cells

Two major advantages of fuel cell-powered vehicles over battery-powered vehicles are longer range and fast fuel refill time. Regardless, the low energy density of hydrogen fuel remains a technical barrier for HDV fuel cells. If one were to consider a typical heavy-duty Class 8 truck, the volume of the fuel and fuel tanks for a diesel internal combustion engine with a 50,000 lbs. load is 795 L, whereas the volume of the fuel and fuel tanks for a compressed hydrogen storage system of a fuel cell is 7,800 L—approximately ten times higher.⁵⁰ If the fuel is replaced by methanol, the volume of the fuel, fuel tanks, and the reformer to store and convert the methanol to hydrogen through reforming is 2,460 L (approximately 30% of the volume equivalent of compressed hydrogen). In addition to volume, working through these same

metrics on the basis of weight, a 50,000 lb. load of cargo would require 1,950 lbs. of diesel and a tank to contain the diesel, or 12,920 lbs. of compressed hydrogen and high-pressure hydrogen tanks, or 7,560 lbs. of methanol, methanol tank, and a reformer capable of producing hydrogen with less than 10 ppm CO. If an intermediate temperature fuel cell stack was employed, the weight and complexity of the reformer drops due to the elimination of the third stage because 2% CO is typically acceptable. Thus, liquid fuels as hydrogen carriers offer a lower impact on load-carrying ability. Liquid fuels significantly reduce the hydrogen infrastructure problem as well. The global infrastructure cost for compressed hydrogen would be \$15 trillion assuming a modest automotive penetration of 200 vehicles per 1,000 inhabitants, while the infrastructure cost for using a renewable liquid fuel such as methanol costs only \$50 billion, or 0.3% of the compressed hydrogen infrastructure cost due to the ability to use or modify existing infrastructure.² The infrastructure for liquid fuel is significantly less expensive than the battery electric vehicle infrastructure that would cost \$5 trillion largely due to a significantly expanded grid capacity. These estimates are based solely on storage and distribution of the fuel, not the cost to make the fuel or electricity. On-board reforming has already been implemented for liquid fuels for commercial systems ranging from tens to thousands of watts, whereby the ease and availability of methanol as a fuel, low-cost reformation, and proven thermal and physical integration with the high temperature fuel cell stack provides customer value. Thus, there is a path to on-board reforming for HDVs.

A challenge for liquid-fueled fuel cells is the need for very fast reforming systems that can compete with hydrogen-based systems in overall specific and volumetric power density. Reformate hydrogen is problematic in LT-PEMFCs as Pt-based catalysts are very sensitive to CO poisoning. Pressure swing CO adsorption and gas-permeable membrane separation require very high pressures for separation and is therefore impractical for transportation applications.⁵¹ One simple solution to resolve the CO issue is to operate fuel cells at high temperatures (>200°C) under which electrode poisoning by CO can be minimized. [Figure 6A](#) shows the current density of a fuel cell at a constant voltage of 0.4 V at 240°C in the presence of CO. The current density loss was 12% (1.14 to 1.0 A cm⁻²) with 25% CO and the performance was completely recovered after pure hydrogen was reintroduced. Current reformer systems coupled with fuel cells include water gas shift reactors to decrease the CO concentration to <10 ppm.

Ideally, the reforming is done at the cell/stack level, that is, internal reforming, thus eliminating an external reformer. This also typically dictates >200°C operational temperature. For example, [Figure 6B](#) shows a solid acid (i.e., CsH₂PO₄) fuel cell stack performance on various liquid and gaseous fuel reformates containing different CO concentrations. The MEAs used in the solid acid fuel cell stack incorporate a methanol steam reforming (MSR) catalyst in front of the hydrogen oxidation electrode. This allows for direct MSR when running on methanol. The MSR layer also acts as a highly efficient CO water gas shift catalyst. As such, the externally reformed fuels, with a CO concentration range from 1%–6%, perform similarly due to nearly 100% CO shifting to H₂ and CO₂ in the presence of water inside the cell.

Three different types of proton conductors have the potential to allow fuel cell operation at >200°C. The first type of candidate materials are ion-pair membranes. As explained earlier, these materials are composed of cation functionalized polymers doped with phosphoric or phosphonic acid. The advantage of these materials is their low ohmic resistance because of their relatively high acid concentration and thin-film separators (~40 μm) ([Figure 6C](#)). Due to their low resistance, the fuel cell power

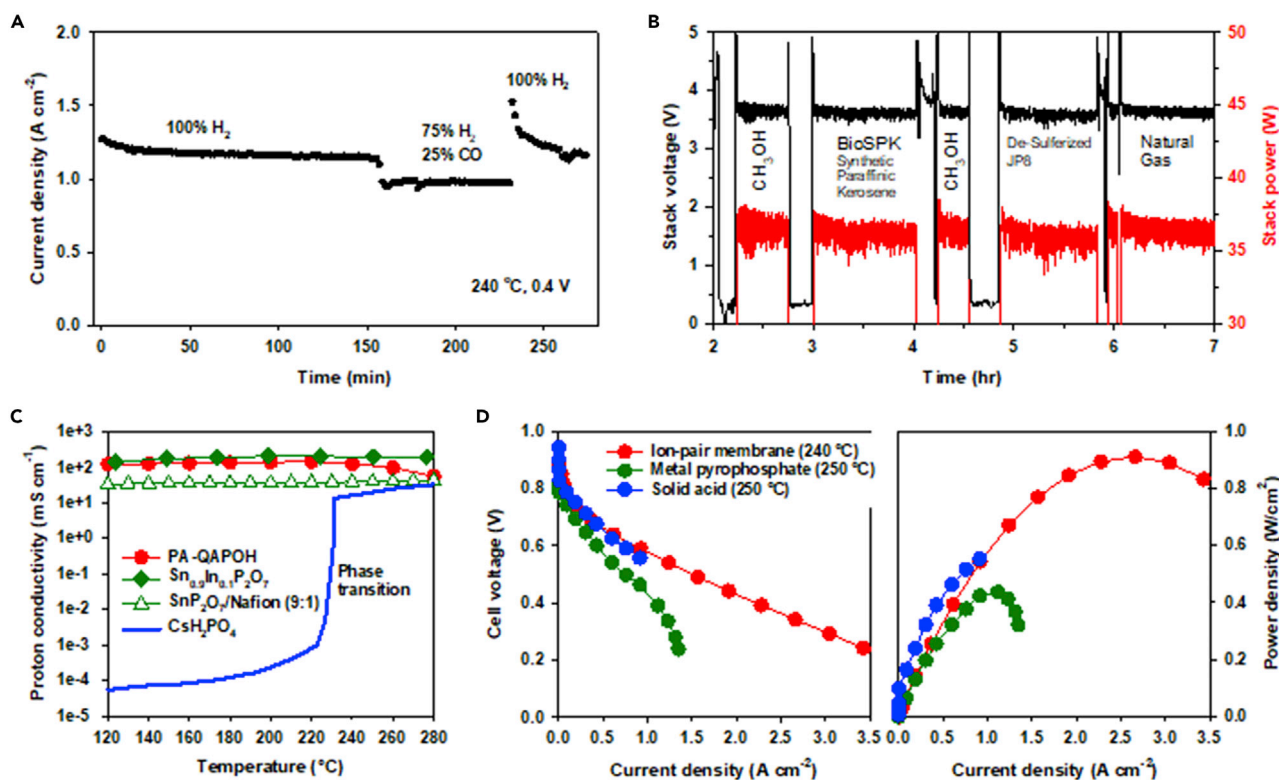


Figure 6. Performance of intermediate temperature fuel cells

(A) Fuel cell performance test using simulated reformat conditions (75% H₂–25% CO) versus O₂. Pt/C (0.6 mg_{Pt} cm⁻²) and phosphoric acid-doped 90 wt % metal pyrophosphate composite membrane (thickness: 100 μm) was used.

(B) Fuel flexibility of fuel cell stacks operate at 250°C. Stack: solid acid fuel cells (5 cell stack, cell active area: ~100 cm², 10 A or 100 mA cm⁻²), Gas flows: cathode: 50% utilization, air with 30% H₂O, Anode: 60%–80% utilization, -reformat 30%–50% H₂O. Gas compositions (dry): CH₃OH – 59% H₂, 1% CO, JP8 (no S) – 38% H₂, 3% CO, BioSPK – 39% H₂, 5% CO, NG – 47% H₂, 6% CO.

(C) Proton conductivity of PA-QAPOH, metal pyrophosphate-based (Sn_{0.9}In_{0.1}P₂O₇, and SnP₂O₇/nafion composite) and solid acid (CsH₂PO₄) electrolytes in the temperature range of 120°C–280°C. The data were taken from Kreller et al.⁵³

(D) H₂/air fuel cell performance of an MEA using an ion-pair polymer, metal pyrophosphate electrolyte and solid acid electrolyte. PEM, PA-QAPOH ion-pair PEM (thickness: 40 μm); ionomer, phosphonated ionomer, anode catalyst, Pt/C (0.6 mg_{Pt} cm⁻²); cathode catalyst, Pt/C (0.6 mg_{Pt} cm⁻²). The performance was measured at 240°C under backpressure of 147 kPa_{abs}. PEM: phosphoric acid-doped SnP₂O₇/nafion (9:1) composite (thickness: 80 μm), ionomer: ion-pair (phosphoric acid-doped quaternary ammonium polystyrene), Anode catalyst: Pt/C (0.6 mg_{Pt} cm⁻²), cathode catalyst, Pt/C (0.6 mg_{Pt} cm⁻²). The performance was measured at 250°C under backpressure of 285 kPa_{abs}. MEA using the solid acid electrolyte. PEM: CsH₂PO₄, (thickness: 50 μm), Anode catalyst: Pt/C (0.6 mg_{Pt} cm⁻²), Cathode catalyst: Pt-Pd alloy (1.3 mg_{Pt} cm⁻²). The performance was measured at 250°C under backpressure of 141 kPa_{abs} and water vapor pressure of 30.4 kPa.

density is relatively high (910 mW cm⁻²) at 240°C under H₂/air conditions (Figure 6D).

There are two technical challenges to utilizing these materials for liquid fuel operations. First, acid loss due to acid evaporation causes cell performance loss over time when the fuel cell operates at >220°C. Second, phosphate poisoning by free acids lowers OCV and kinetic performance. Phosphonic acids with low vapor pressure and minimal poisoning to fuel cell electrodes may need to be developed.

The second candidate material is a metal pyrophosphate (MP₂O₇, where M = Sn, Ti, Zr, W, Ce, Si, Ge). Indium-doped tin pyrophosphate (Sn_{0.9}In_{0.1}P₂O₇) exhibited a proton conductivity of 195 mS cm⁻¹ at 250°C.⁵² Recent studies on metal-doped and undoped tin pyrophosphates have shown that the crystalline phase itself possesses negligible protonic conductivity. However, the presence of an excess amorphous polyphosphate phase is key for achieving high proton conductivity.⁵³ The advantage of these materials is stability and high conductivity over a wide temperature range

(100°C–250°C). However, making a thin-film separator is challenging due to the brittle nature of the metal pyrophosphate particles. Therefore, the electrolyte separator was prepared from a polymer composite with 90 wt % SnP_2O_7 and 10 wt % Nafion (<100 μm -thick membrane separator). Although the proton conductivity of the composite membrane was 40% of the SnP_2O_7 pellets (80 mS cm^{-1} at 250°C) (Figure 6C),⁵⁴ the cell's resistance can be reduced by using a thin composite membrane. Reasonably high H_2 /air performance (peak power density = 440 mW cm^{-2} at 250°C) was reported (Figure 6D).

The third candidate material is a solid acid electrolyte. The general formula of the solid acid is $\text{M}_x\text{H}_y(\text{XO}_4)_z$ ($\text{M} = \text{Cs, Rb, K, NH}_4, \text{X} = \text{S, Se, P, As}$).^{55–57} At low temperatures (<200°C), these materials are brittle, gas-permeable, water-soluble, and poor proton conductors. However, at high temperatures, these materials undergo a phase transition to a higher symmetry “super-protonic” phase to possess plastic-like properties leading to gas impermeable membranes and a reasonably high proton conductivity (ca. 20 mS cm^{-1} at 250°C). As the super-protonic phases of solid acids are typically at 140°C–260°C, water solubility issues can be avoided, as water will be in the form of steam and can easily be removed upon cooling down. Figure 6C shows the proton conductivity of CsH_2PO_4 as a function of temperature. As noted, the phase transition occurred at $\sim 230^\circ\text{C}$ above which proton conductivity jumped to >10 mS cm^{-1} .⁵⁸ CsH_2PO_4 is thermodynamically stable as a solid at temperatures up to 300°C with proper hydration.⁵⁹ This enables electrocatalyst particles to be deposited directly on the surface of sub-micron CsH_2PO_4 particles in the electrodes. Such an electrode, with Pt-Pd alloy nanoparticle resting on CsH_2PO_4 electrolyte particles used as a cathode for ORR exhibits viable performance (Figure 6D).⁶⁰ Combined with the high impurity tolerances of the anode Pt/C catalyst and the ability to incorporate internal chemical catalysts for various reactions (e.g., steam reforming, CO water gas shift, ammonia decomposition, dehydrogenation), solid acid stacks can run on a wide variety of liquid fuels and reformat streams with no or minimal reforming sub-system, greatly reducing system-level complexity and costs. The drawback of CsH_2PO_4 proton conductors is their requirement for proper hydration (from 0.2 atm at 230°C to 0.3 atm at 250°C to 0.6 atm at 280°C to 1 atm at 300°C) to keep the solid acid from dehydrating to CsPO_3 . Thus, hydration sub-systems for both the anode and cathode are normally needed. Also, the “plastic-like” nature of the electrolyte particles, which is beneficial in the membrane as they sinter gas-tight at operational temperatures, results in densification at the electrodes, causing increased mass transport losses.

OUTLOOK

Table 1 summarizes the performance and durability of fuel cells employing current proton conductors for HDV applications. Proton conductors for LT-PEMFCs are a mature technology with near-term durability challenges. Proton conductors for HT-PEMFCs are an emerging technology that provide the benefits of simpler heat and water management for HDV fuel cells. Proton conductors for intermediate temperature fuel cells provide an attractive solution with liquid-fuel utilization. In this section, we discuss the most critical challenges, opportunities, and future research directions of proton conductors for HDV fuel cell applications.

Proton conductors for LT-PEMFCs

Designing highly conductive and robust PFSA membranes has been a central subject for automotive LT-PEMFCs. Therefore, various strategies are available, including adjusting the length of side chains, incorporating inorganic fillers, polymer blends, and

Table 1. Fuel cell performance and durability employing current proton conductors

Approach	LT-PEMFC ¹⁵		HT-PEMFC				Intermediate temperature fuel cell		
			PA-PBI ^{40,60}		Ion-pair ⁴⁹		Metal P ₂ O ₇ ⁵⁵	Solid acid	
Temperature range (°C)	65–95		140–200		80–240		200–240	220–260	
Water vapor pressure (kPa)	4–100		0–10		0–20		not available	0–40	
Lifetime (hours)	20,000 at 80°C ^a		>17,000 at 160°C ^b		>550 at 160°C ^c		not available	900°C at 220°C ^d	>8,000 at 250°C ^e
Power density (mW cm ⁻²)	at 0.7 V	840	120 at 80°C		80 at 160°C		230 at 240°C	120 at 240°C	340 at 250°C
	rated	380	450		480		910	430	440
	peak	1,400	450		550				

^aProjected from AST equivalent.

^bDemonstrated at a constant current density of 0.2 A cm⁻² with voltage decay rate of 5 μV h⁻¹.

^cDemonstrated at a constant current density of 0.6 A cm⁻² with voltage decay rate of 0.35 μV h⁻¹.

^dDemonstrated at a constant voltage of 0.5 V (Figure S1).

^eProjected at a constant current density of 0.2 A cm⁻² with 20% voltage degradation (Figure S2).

multi-acid side chains.⁶¹ The current reinforcement technology is able to reduce the membrane thickness to less than 10 μm. Today, membranes for LDV fuel cells are typically less than 20 μm with the Toyota Mirai using a 10 μm thick PFSA membrane. For HDV applications, these PFSA-technologies can be fully transferable as the cell resistance requirement remains the same. However, further consideration regarding a more stringent durability requirement needs to be addressed. Better mechanical stability is obtainable by implementing thicker membranes (>20 μm), which can be effectively produced with low cost by using melt extrusion processes.²⁸ Enhancing chemical stability by immobilizing radical scavengers is an on-going research subject. For alternative hydrocarbon membrane chemistries, improving mechanical properties under wet-dry cycling conditions while simultaneously meeting performance requirements is essential to enable these material systems for HDV applications. Sulfonated polyolefinic membranes may resolve the mechanical instability issue, but other requirements such as thermal-oxidative stability and conductivity at low RHs need to be verified.⁶² Mechanical reinforcement and introducing flexible moieties for sulfonated polyaromatics are possible approaches.^{30,63}

Proton conductors for HT-PEMFCs

The development of proton conductors having high conductivity under hot and dry conditions has shown notable progress over the last five years and shows promise in overcoming the limitations of LT-PEMFCs when operating in these environments. The field of HT-PEMFCs continues to progress in the United States, Europe, and Asia. The European Space Agency (ESA) has funded several programs to take HT-PEMFC stacks into space to power satellites and vehicles on the moon due to their superior heat rejection, which is highly desired in a vacuum environment.⁶⁴ In China, PBI-based MEAs are being used in systems with on-board methanol reforming to charge the batteries of small truck electric vehicles.⁶⁵ To enable HT-PEMFCs for HDV applications, a number of studies have been devoted to improving acid retention in the presence of water by incorporating inorganic fillers,⁶⁶ cross-linking,⁶⁷ and enhanced interaction with phosphoric acid dopants.^{68,69} Recently, metal-organic frameworks^{70,71} and covalent organic frameworks^{72,73} with phosphoric acid proton carriers were proposed as anhydrous proton conductors. However, there are limited studies on the fuel cell's performance and durability, both of which are vital for advancing these materials for practical HDV fuel cell applications. The most promising approach for HDV applications that showed high acid retention under automotive operating conditions is ion-pair membranes.^{74,75}

Stable performance of ion-pair-based HT-PEMFCs was demonstrated at a moderate, steady current density (0.6 A cm^{-2}), high stoichiometric flows (>10), and under humidified conditions ($P_{\text{H}_2\text{O}} = 10 \text{ kPa}$). Additional performance and durability validation at low operating temperatures ($\sim 80^\circ\text{C}$), on/off cycling, and dynamic load conditions are required. There remain many opportunities to optimize ion-pair membranes for HDV applications. Specifically, the correlations between different types of ion-pairs, acid retention capability, and mechanical properties of acid plasticized and ionically cross-linked membranes are largely unexplored. Questions regarding membrane stability under water-free, higher temperature, frequent start/stop cycles, and radical-generating conditions require further investigation. These questions present many technical challenges and opportunities for researchers to develop affordable PEMs for HDV applications. Developing highly performing ionomeric binders for HT-PEMFCs is another pressing technical challenge as most HT-PEMFCs show much lower fuel cell performance than PFSA-based LT-PEMFCs. For PA-PBI-based HT-PEMFCs, only PTFE-type binders perform well due to prevention of electrode flooding by phosphoric acid. However, for ion-pair membrane-based HT-PEMFCs, electrode flooding is less worrisome because the dopant level of phosphoric acid in membranes is lower, suggesting that there is room for designing more advanced ionomers based on phosphonic acids or other proton conductors. Fundamental studies on catalyst-ionomer interactions, gas transport, and proton conductivity at the catalyst-ionomer interface are essential to develop a well-performing HT-PEMFC system. Innovative ideas to minimize phosphate anion poisoning of cathode catalysts are necessary to achieve high kinetic performance. These efforts have been primarily relegated to catalyst developers, but the design of the ionomeric binder plays a critical role as well.

Proton conductors for liquid-fueled fuel cells

Fuel cells that operate $>200^\circ\text{C}$ are attractive as future technologies enable the use of liquid fuels through direct *in situ* reformat processes. The intrinsic advantage of intermediate temperature fuel cells that can operate with various high energy density liquid fuels is the flexibility to run in various geographical regions that may have natural availability of one fuel over another. Several materials that have high proton conductivity have been developed. The performance and durability of these proton conductors still need to be demonstrated in MEA configurations to enable commercially viable systems. Thermal stability of stack and MEA components and cell durability remain challenges for HDV applications. While, “hotter is better,” is the generally accepted belief in the case of high-temperature membranes, there are additional challenges for running “hotter.” For example, while the potential of directly oxidizing fuel at the anode has benefits, this mode runs the risk of lower reaction yields compared with a more complete reforming in systems with independent reformers and fuel cells. Therefore, highly active catalysts and electrode designs for optimum mass transport are needed.⁷⁶ Another challenge of running too hot is finding appropriate materials for MEA and cell construction. Running over a temperature of 260°C eliminates most polymers and running at 300°C restricts options to the most expensive gasket materials with unproven operation over 10,000 h. Similarly, running at 250°C with unbound conducting elements, such as phosphoric acid absorbed in a matrix, could be difficult due to their volatility. However, for simple fuels such as methanol, 220°C is a reasonable temperature to match is needed for the complete thermal integration of the fuel cell and the reformer. Bipolar plates have additional challenges when operating at higher temperatures. However, in a low/no water environment, bipolar plates could be freed from other material constraints associated with the liquid

water environments of LT-PEMFCs, such as corrosion, thus potentially enabling stamped metal bipolar plates. In addition, polymer seal material options at $>200^{\circ}\text{C}$ are limited and typically expensive. Furthermore, typical carbon-supported Pt-group metal (PGM) ORR catalysts, which have allowed for low PGM loadings with high catalytic activity, are not sufficiently robust to withstand carbon corrosion above 200°C . As such, all $>200^{\circ}\text{C}$ liquid-fueled fuel cells will need to search for corrosion-resistant cathode catalysts to enable lifetimes sufficient for HDVs with low PGM loadings.

In conclusion, proton conductors play a pivotal role in HDV fuel cell applications. PFSA is a mature technology that needs substantial improvement of chemical and mechanical stability to meet the rigorous HDV durability requirements under increased stress compared with LDVs. Phosphoric acid-doped polymer electrolytes are emerging with better acid retention in the presence of water, although further stability validation under dynamic automotive load and startup/shutdown cycles is required. Proton conductors at the intermediate temperature range (200°C – 260°C) enable direct operation using hydrocarbon syngas, reformates, and simple liquid fuels such as methanol, formic acid, and dimethyl ethers. Such fuel cells require highly conductive membranes and low-cost electrodes as well as high material stability at these operating conditions. Other types of fuel cells also have potential for HDV applications, albeit with greater technical challenges. Alkaline anion exchange membrane fuel cells have exhibited high performance,^{77–79} but improvement in durability, particularly with PGM-free catalysts, remains a major challenge.⁸⁰ Protonic ceramic fuel cells have demonstrated high electrical efficiency with direct feed of hydrocarbon fuels, but high operating temperatures ($>500^{\circ}\text{C}$) limit their use for primary electrical power systems for transportation applications.^{81,82} All the challenges discussed in this article incentivize more focused research toward future heavy-duty electrification as fuel cells are perhaps the most promising enabler for replacing current ICEs with high efficiency and environmental-friendly systems.

SUPPLEMENTAL INFORMATION

Supplemental information can be found online at <https://doi.org/10.1016/j.joule.2021.05.016>.

ACKNOWLEDGMENTS

This work was supported by the US Department of Energy, Energy Efficiency and Renewable Energy, Hydrogen and Fuel Cell Technologies Office (HFTO) (M2FCT consortia, Technology Managers: G. Kleen and D. Papageorgopoulos) and Advanced Research Project Agency-Energy (ARPA-E) (award number: DE-AR0001003, Program Director: Grigori Soloveichik). Los Alamos National Laboratory is operated by Triad National Security, LLC under U. S. Department of Energy contract number 89233218CNA000001.

AUTHOR CONTRIBUTIONS

Y.S.K. proposed the idea. All authors wrote the manuscript.

DECLARATION OF INTERESTS

The authors declare no competing interests.

REFERENCES

1. Miller, E.L., Thompson, S.T., Randolph, K., Hulvey, Z., Rustagi, N., and Satyapal, S. (2020). US Department of Energy hydrogen and fuel cell technologies perspectives. *MRS Bull* 45, 57–64.
2. Shih, C.F., Zhang, T., Li, J., and Bai, C. (2018). Powering the future with liquid sunshine. *Joule* 2, 1925–1949.
3. Kauw, M., Benders, R.M.J., and Visser, C. (2015). Green methanol from hydrogen and carbon dioxide using geothermal energy and/or hydropower in Iceland or excess renewable electricity in Germany. *Energy* 90, 208–217.
4. Ray, A., and Anumakonda, A. (2011). Production of green liquid hydrocarbon fuels. *Biofuels, Alternative Feedstocks and Conversion Processes* (Academic Press), pp. 587–608.
5. Panahi, H.K.S., Dehghani, M., Kinder, J.D., and Ezeji, T.C. (2019). A review on green liquid fuels for the transportation sector: a prospect of microbial solutions to climate change. *Biofuel Res. J.* 23, 995–1024.
6. Adams, J. (2020). DOE H2 heavy duty truck Targets. Compressed Gas Storage for Medium and Heavy Duty Transportation Workshop (University of Sayton Research Institute), p. 45469. <https://www.energy.gov/sites/prod/files/2020/02/f71/fcto-compressed-gas-storage-workshop-2020-adams.pdf>.
7. Ahluwalia, R.K., Wang, X., and Steinbach, A.J. (2016). Performance of advanced automotive fuel cell systems with heat rejection constraint. *J. Power Sources* 309, 178–191.
8. Pei, P., Wang, M., Chen, D., Ren, P., and Zhang, L. (2020). Key technologies for polymer electrolyte membrane fuel cell systems fueled impure hydrogen. *Progress in Natural Science: Materials International* 30, 751–763.
9. Steck, A. (1995). In *Proceeding 1st International Symposium. New Materials for Fuel Cell Systems*, O. Savagodo, P.R. Roberge, and T.N. Veziroglu, eds., p.74.
10. Lim, C., Ghassemzadeh, L., Van Hove, F., Lauritzen, M., Kolodziej, J., Wang, G.G., Holdcroft, S., and Kjeang, E. (2014). Membrane degradation during combined chemical and mechanical accelerated stress testing of polymer electrolyte fuel cells. *J. Power Sources* 257, 102–110.
11. Lai, Y.H., and Fly, G.W. (2015). In-situ diagnostics and degradation mapping of a mixed-mode accelerated stress test for proton exchange membranes. *J. Power Sources* 274, 1162–1172.
12. Gittleman, C.S., Coms, F.D., and Lai, Y.-H. (2012). Membrane durability: physical and chemical degradation. In *Modern Topics in Polymer Electrolyte Fuel Cell Degradation*, M. Mench, E.C. Kumbur, and T.N. Veziroglu, eds. (Academic Press), pp. 15–88.
13. Robert, M., El Kaddouri, A., Perrin, J.C., Mozet, K., Daoudi, M., Dillet, J., Morel, J.Y., André, S., and Lottin, O. (2020). Effects of conjoint mechanical and chemical stress on perfluorosulfonic-acid membranes for fuel cells. *J. Power Sources* 476, 228662.
14. Mukundan, R., Baker, A.M., Kusoglu, A., Beattie, P., Knights, S., Weber, A.Z., and Borup, R.L. (2018). Membrane accelerated stress test development for polymer electrolyte fuel cell durability validated using field and drive cycle testing. *J. Electrochem. Soc.* 165, F3085–F3093.
15. Ramaswamy, N. (2020). Durable fuel cell MEA through immobilization of catalyst particle and membrane chemical stabilizer. US DOE Hydrogen and Fuel Cells Program: 2020 Annual Merit Review and Peer Evaluation Report. https://www.hydrogen.energy.gov/pdfs/review20/fc323_ramaswamy_2020_p.pdf.
16. Lai, Y.-H., Rahmoeller, K.M., Hurst, J.H., Kukreja, R.S., Atwan, M., Maslyn, A.J., and Gittleman, C.S. (2018). Accelerated stress testing of fuel cell membranes subjected to combined mechanical/chemical stressors and cerium migration. *J. Electrochem. Soc.* 165, F3217–F3229.
17. Zatoń, M., Rozière, J., and Jones, D.J. (2017). Current understanding of chemical degradation mechanisms of perfluorosulfonic acid membranes and their mitigation strategies: a review. *Sustainable Energy Fuels* 1, 409–438.
18. D'Urso, C., Oldani, C., Baglio, V., Merlo, L., and Ario, A.S. (2017). Fuel cell performance and durability investigation of bimetallic radical scavengers in Aquivion perfluorosulfonic acid membranes. *International Journal of Hydrogen Energy* 42, 27987–27994.
19. Motz, A.R., Kuo, M.-C., Horan, J.L., Yadav, R., Seifert, S., Pandey, T.P., Galioto, S., Yang, Y., Dale, N.V., Hamrock, S.J., and Herring, A.M. (2018). Heteropoly acid functionalized fluoroelastomer with outstanding chemical durability and performance for vehicular fuel cells. *Energy Environ. Sci.* 11, 1499–1509.
20. Zatoń, M., Prélôt, B., Donzel, N., Rozière, J., and Jones, D.J. (2018). Migration of Ce and Mn ions in PEMFC and its impact on PFSA membrane degradation. *J. Electrochem. Soc.* 165, F3281–F3289.
21. Baker, A.M., Mukundan, R., Spornjak, D., Judge, E.J., Advani, S.G., Prasad, A.K., and Borup, R.L. (2016). Cerium migration during PEM fuel cell accelerated stress testing. *J. Electrochem. Soc.* 163, F1023–F1031.
22. Trogadas, P., Parrondo, J., and Ramani, V. (2008). Degradation mitigation in polymer electrolyte membranes using cerium oxide as a regenerative free-radical scavenger. *Electrochem. Solid-State Lett.* 11, B113.
23. Pearman, B.P., Mohajeri, N., Brooker, R.P., Rodgers, M.P., Slatery, D.K., Hampton, M.D., Cullen, D.A., and Seal, S. (2013). The degradation mitigation effect of cerium oxide in polymer electrolyte membranes in extended fuel cell durability tests. *J. Power Sources* 225, 75–83.
24. Baker, A.M., Williams, S.T.D., Mukundan, R., Spornjak, D., Advani, S.G., Prasad, A.K., and Borup, R.L. (2017). Zr-doped ceria additives for enhanced PEM fuel cell durability and radical scavenger stability. *J. Mater. Chem. A* 5, 15073–15079.
25. Baker, A.M., Stewart, S.M., Ramaiyan, K.P., Banham, D., Ye, S., Garzon, F., Mukundan, R., and Borup, R.L. (2021). Doped ceria nanoparticles with reduced solubility and improved peroxide decomposition activity for PEM fuel cells. *J. Electrochem. Soc.* 168, 024507.
26. Zhang, Z., Shi, S.W., Lin, Q., Wang, L., Liu, Z., Li, P.Z., and Chen, X. (2018). Exploring the role of reinforcement in controlling fatigue crack propagation behavior of perfluorosulfonic-acid membranes. *International Journal of Hydrogen Energy* 43, 6379–6389.
27. Li, Y., Jiang, R., and Gittleman, C.S. (2020). Effects of melt flow index and equivalent weight on the dimensional stability and mechanical behavior of perfluorosulfonic acid ionomer membranes. *J. Power Sources* 478, 228734.
28. Gittleman, C.S., Coms, F.D., and Lai, Y.-H. Low temperature PEM degradation: failure modes & mitigation strategies. 225th Meeting of Electrochemical Society. <https://ecs.confex.com/ecs/225/webprogram/Paper30925.html>.
29. Hickner, M.A., Ghassemi, H., Kim, Y.S., Einsla, B.R., and McGrath, J.E. (2004). Alternative polymer systems for proton exchange membranes (PEMs). *Chem. Rev.* 104, 4587–4611.
30. Miyake, J., Taki, R., Mochizuki, T., Shimizu, R., Akiyama, R., Uchida, M., and Miyatake, K. (2017). Design of flexible polyphenylene proton-conducting membrane for next-generation fuel cells. *Sci. Adv.* 3, ea00476.
31. Kim, Y.S. (2021). Polymer electrolytes with high ionic concentration for fuel cells and electrolyzers. *ACS Appl. Polym. Mater.* 3, 1250–1270.
32. MacKinnon, S.M., Fuller, T.J., Coms, F.D., Schoeneweiss, M.R., Gittleman, C.S., Lai, Y.-H., Jiang, R., and Brenner, A. (2009). Design and characterization of alternative proton exchange membranes for automotive applications. In *Encyclopedia of Electrochemical Power Sources*, J. Garche, C.K. Dyer, P.T. Moseley, Z. Ojumi, D.A.J. Rand, and B. Scrosati, eds. (Elsevier), pp. 741–754.
33. Jiang, R., Fuller, T.J., Brawn, S., and Gittleman, C.S. (2013). Perfluorocyclobutane and poly(vinylidene fluoride) blend membranes for fuel cells. *Electrochim. Acta* 110, 306–315.
34. Ishikawa, H., Teramoto, T., Ueyama, Y., Sugawara, Y., Sakiyama, Y., Kusakabe, M., Miyatake, K., and Uchida, M. (2016). Use of a sub-gasket and soft gas diffusion layer to mitigate mechanical degradation of a hydrocarbon membrane for polymer electrolyte fuel cells in wet-dry cycling. *J. Power Sources* 325, 35–41.
35. Mathias, M.F., Makharia, R., Gasteiger, H.A., Conley, J.J., Fuller, T.J., Gittleman, C.S., Kocha, S.S., Miller, D.P., Mittelsteadt, C.K., Xie, T., et al. (2005). Two fuel cell cars in every garage? *Electrochem. Soc. Interface* 14, 24–35.
36. Gubler, L., Nauser, T., Coms, F.D., Lai, Y.-H., and Gittleman, C.S. (2018). Perspective - prospects for durable hydrocarbon-based fuel

- cell membranes. *J. Electrochem. Soc.* **165**, F3100–F3103.
37. Suzuki, T., Iiyama-Kubo, A., Saito, N.N., Shinohara, K., Shimotori, S., et al. Towards future fuel cell -Challenge for 2040. 236th Meeting of Electrochemical Society. Abstract No. I01Z-1763. <https://ecs.confex.com/ecs/236/meetingapp.cgi/Paper/125808>.
 38. Vinothkannan, M., Kim, A.R., Gnana kumar, G.G., and Yoo, D.J. (2018). Sulfonated graphene oxide/nafiion composite membranes for high temperature and low humidity proton exchange membrane fuel cells. *RSC Adv* **8**, 7494–7508.
 39. Park, C.H., Lee, S.Y., Hwang, D.S., Shin, D.W., Cho, D.H., Lee, K.H., Kim, T.-W., Kim, T.-W., Lee, M., Kim, D.-S., et al. (2016). Nanocrack-regulated self-humidifying membranes. *Nature* **532**, 480–483.
 40. Pingitore, A.T., Huang, F., Qian, G., and Benicewicz, B.C. (2019). Durable high polymer content m / p-polybenzimidazole membranes for extended lifetime electrochemical devices. *ACS Appl. Energy Mater.* **2**, 1720–1726.
 41. Kannan, A., Aili, D., Cleemann, L.N., Li, Q., and Jensen, J.O. (2020). Three-layered electrolyte membranes with acid reservoir for prolonged lifetime of high-temperature polymer electrolyte membrane fuel cells. *International Journal of Hydrogen Energy* **45**, 1008–1017.
 42. Søndergaard, T., Cleemann, L.N., Zhong, L., Becker, H., Steenberg, T., Hjuler, H.A., Seerup, L., Li, Q., and Jensen, J.O. (2018). Catalyst degradation under potential cycling as an accelerated stress test for PBI-based high-temperature PEM fuel cells - Effect of humidification. *Electrocatalysis* **9**, 302–313.
 43. Lee, A.S., Choe, Y.K., Matanovic, I., and Kim, Y.S. (2019). The energetics of phosphoric acid interactions reveals a new acid loss mechanism. *J. Mater. Chem. A* **7**, 9867–9876.
 44. Lee, K.S., Spendelow, J.S., Choe, Y.K., Fujimoto, C., and Kim, Y.S. (2016). An operationally flexible fuel cell based on quaternary ammonium-bisphosphate ion pairs. *Nat. Energy* **1**, 16120.
 45. Ghoshal, S., Jia, Q., Bates, M.K., Li, J., Xu, C., Gath, K., Yang, J., Waldecker, J., Che, H., Liang, W., et al. (2017). Tuning Nb-Pt interactions to facilitate fuel cell electrocatalysis. *ACS Catal* **7**, 4936–4946.
 46. Li, Q., Wu, G., Cullen, D.A., More, K.L., Mack, N.H., Chung, H.T., and Zelenay, P. (2014). Phosphate-tolerant oxygen reduction catalysts. *ACS Catal* **4**, 3193–3200.
 47. Gan, F., and Chin, D.-T. (1993). Determination of diffusivity and solubility of oxygen in phosphoric-acid using a transit-time on a rotating ring-disc electrode. *J. Appl. Electrochem.* **23**, 452–455.
 48. Eberhardt, S.H., Toulec, M., Marone, F., Stampanoni, M., Büchi, F.N., and Schmidt, T.J. (2015). Dynamic operation of HT-PEFC: in-operando imaging of phosphoric acid profiles and (re)distribution. *J. Electrochem. Soc.* **162**, F310–F316.
 49. Atanasov, V., Lee, A.S., Park, E.J., Maurya, S., Baca, E.D., Fujimoto, C., Hibbs, M., Matanovic, I., Kerres, J., and Kim, Y.S. (2021). Synergistically integrated phosphonated poly(pentafluorostyrene) for fuel cells. *Nat. Mater.* **20**, 370–377.
 50. Chan, T. (2020). Methanol fuel cells: powering the future. Methanol institute. Element 1 Corp presentation. <https://3xngg2wmai7100rss2cgkmj-wpengine.netdna-ssl.com/wp-content/uploads/2020/04/Methanol-Fuel-Cell-Powering-the-Future-webinar-presentation.pdf>.
 51. Amphlett, J.C., Creber, K.A.M., Davis, J.M., Mann, R.F., Peppley, B.A., and Stokes, D.M. (1994). Hydrogen production by steam reforming of methanol for polymer electrolyte fuel cells. *International Journal of Hydrogen Energy* **19**, 131–137.
 52. Nagao, M., Kamiya, T., Heo, P., Tomita, A., Hibino, T., and Sano, M. (2006). Proton conduction in In³⁺-doped SnP₂O₇ at intermediate temperatures. *J. Electrochem. Soc.* **153**, A1604–A1609.
 53. Kreller, C.R., Pham, H.H., Wilson, M.S., Mukundan, R., Henson, N., Sykora, M., Hartl, M., Daemen, L., and Garzon, F.H. (2017). Intragranular phase proton conduction in crystalline Sn_{1-x}In_xP₂O₇ (x=0 and 0.1). *J. Phys. Chem. C* **121**, 23896–23905.
 54. Lee, K.S., Maurya, S., Kim, Y.S., Kreller, C.R., Wilson, M.S., Larsen, D., Elangovan, S.E., and Mukundan, R. (2018). Intermediate temperature fuel cells via an ion-pair coordinated polymer electrolyte. *Energy Environ. Sci.* **11**, 979–987.
 55. Haile, S.M., Boysen, D.A., Chisholm, C.R.I., and Merle, R.B. (2001). Solid acids as fuel cell electrolytes. *Nature* **410**, 910–913.
 56. Haile, S.M., Chisholm, C.R.I., Sasaki, K., Boysen, D.A., and Uda, T. (2007). Solid acid proton conductors: from laboratory curiosities to fuel cell electrolytes. *Faraday Discuss* **134**, 17–39.
 57. Ward, M.D., Chaloux, B.L., Michelle, C., Johannes, D., and Epshteyn, A. (2020). Facile proton transport in ammonium Borosulfate – an unhumidified solid acid polyelectrolyte for intermediate temperatures. *Adv. Mater.* **32**, 2003667.
 58. Boysen, D.A., Uda, T., Chisholm, C.R.I., and Haile, S.M. (2004). High-performance solid acid fuel cells through humidity stabilization. *Science* **303**, 68–70.
 59. Papandrew, A.B., Chisholm, C.R.I., Zecevic, S.K., Veith, G.M., and Zawodzinski, T.A. (2013). Activity and evolution of vapor deposited Pt-Pd oxygen reduction catalysts for solid acid fuel cells. *J. Electrochem. Soc.* **160**, F175–F182.
 60. De Castro, E. (2009). PBI-phosphoric acid based membrane electrode assemblies: status update, PAFC Workshop. <https://www.energy.gov/eere/fuelcells/downloads/pbi-phosphoric-acid-based-membrane-electrode-assemblies-status-update>.
 61. Kusoglu, A., and Weber, A.Z. (2017). New insights into perfluorinated sulfonic-acid ionomers. *Chem. Rev.* **117**, 987–1104.
 62. Trigg, E.B., Gaines, T.W., Maréchal, M., Moed, D.E., Rannou, P., Wagener, K.B., Stevens, M.J., and Winey, K.I. (2018). Self-assembled highly ordered acid layers in precisely sulfonated polyethylene produce efficient proton transport. *Nat. Mater.* **17**, 725–731.
 63. Miyake, J., Kusakabe, M., Tsutsumida, A., and Miyatake, K. (2018). Remarkable reinforcement effect in sulfonated aromatic polymers as fuel cell membrane. *ACS Appl. Energy Mater.* **1**, 1233–1238.
 64. Casini, A.E.M., Mittler, P., Cowley, A., Schlüter, L., Faber, M., Fischer, B., Wiesche, Mvd, and Maurer, M. (2020). Lunar analogue facilities development at EAC: the LUNA project. *J. Space Saf. Eng.* **7**, 510–518.
 65. Yongjun, G., Liu, J.L., and Bashir, S. (2020). Electrocatalysts for direct methanol fuel cells to demonstrate China's renewable energy renewable portfolio standards within the framework of the 13th five-year plan. *Catal Today*. <https://doi.org/10.1016/j.cattod.2020.10.004>.
 66. Lee, S., Seo, K., Ghorpade, R.V., Nam, K.H., and Han, H. (2020). High temperature anhydrous proton exchange membranes based on chemically-functionalized titanium/polybenzimidazole composites for fuel cells. *Mater. Lett.* **263**, 127167.
 67. Oono, Y., Sounai, A., and Hori, M. (2013). Prolongation of lifetime of high temperature proton exchange membrane fuel cells. *J. Power Sources* **241**, 87–93.
 68. Jang, J., Kim, D.H., Ahn, M.K., Min, C.M., Lee, S.B., Byun, J., Pak, C., and Lee, J.S. (2020). Phosphoric acid doped triazole-containing cross-linked polymer electrolytes with enhanced stability for high-temperature proton exchange membrane fuel cells. *J. Membr. Sci.* **595**, 117508.
 69. Zhou, S.Y., Guan, J.Y., Li, Z.Q., Huang, L., Zheng, J.F., Li, S.H., and Zhang, S.B. (2021). Alkaline polymers of intrinsic microporosity: high-conduction and low-loss anhydrous proton exchange membranes for energy conversion. *J. Mater. Chem. A* **9**, 3925–3930.
 70. Gui, D., Dai, X., Tao, Z., Zheng, T., Wang, X., Silver, M.A., Shu, J., Chen, L., Wang, Y., Zhang, T., et al. (2018). Unique proton transportation pathway in a robust inorganic coordination polymer leading to intrinsically high and sustainable anhydrous proton conductivity. *J. Am. Chem. Soc.* **140**, 6146–6155.
 71. Xing, X.-S., Fu, Z.-H., Zhang, N.-N., Yu, X.-Q., Wang, M.-S., and Guo, G.-C. (2019). High proton conduction in an excellent water-stable gadolinium metal-organic framework. *Chem. Commun.* **55**, 1241–1244.
 72. Tao, S., Zhai, L., Dinga Wankanke, A.D., Addicoat, M.A., Jiang, Q., and Jiang, D. (2020). Confining H₃PO₄ network in covalent organic frameworks enables proton super flow. *Nat. Commun.* **11**, 8191.
 73. Zhou, B., Le, J., Cheng, Z., Zhao, X., Shen, M., Xie, M., Hu, B., Yang, X., Chen, L., and Chen, H. (2020). Simple transformation of covalent organic frameworks to highly proton-conductive electrolytes. *ACS Appl. Mater. Interfaces* **12**, 8198–8205.
 74. Liu, F., Wang, S., Wang, D., Liu, G., Cui, Y., Liang, D., Wang, X., Yong, Z., and Wang, Z. (2021). Multifunctional poly(ionic liquid)s cross-linked polybenzimidazole membrane with

- excellent long-term stability for high temperature-proton exchange membranes fuel cells. *J. Power Sources* 494, 229732.
75. Venugopalan, G., Chang, K., Nijoka, J., Livingston, S., Geise, G.M., and Arges, C.G. (2020). Stable and highly conductive polycation-polybenzimidazole membrane blends for intermediate temperature polymer electrolyte membrane fuel cells. *ACS Appl. Energy Mater.* 3, 573–585.
76. Lohmann-Richters, F.P., Abel, B., and Varga, Á. (2018). In situ determination of the electrochemically active platinum surface area: key to improvement of solid acid fuel cells. *J. Mater. Chem. A* 6, 2700–2707.
77. Maurya, S., Noh, S., Matanovic, I., Park, E.J., Narvaez Villarrubia, C.N., Martinez, U., Han, J., Bae, C., and Kim, Y.S. (2018). Rational design of polyaromatic ionomers for alkaline membrane fuel cells with $>1 \text{ W cm}^{-2}$ power density. *Energy Environ. Sci.* 11, 3283–3291.
78. Wang, J.H., Zhao, Y., Setzler, B.P., Rojas-Carbonell, S., Ben Yehuda, C., Amel, A., Page, M., Wang, L., Hu, K., Shi, L., et al. (2019). Poly(aryl piperidinium) membranes and ionomers for hydroxide exchange membrane fuel cells. *Nat. Energy* 4, 392–398.
79. Mandal, M., Huang, G., Hassan, N.U., Mustain, W.E., and Kohl, P.A. (2020). Poly(norbornene) anion conductive membranes: homopolymer, block copolymer and random copolymer properties and performance. *J. Mater. Chem. A* 8, 17568–17578.
80. Mustain, W.E., Chatenet, M., Page, M., and Kim, Y.S. (2020). Durability challenges of anion exchange membrane fuel cells. *Energy Environ. Sci.* 13, 2805–2838.
81. Choi, S., Kucharczyk, C.J., Liang, Y.G., Zhang, X.H., Takeuchi, I., Ji, H.-I., and Haile, S.M. (2018). Exceptional power density and stability at intermediate temperatures in protonic ceramic fuel cells. *Nat. Energy* 3, 202–210.
82. An, H., Lee, H.-W., Kim, B.-K., Son, J.-W., Yoon, K.J., Kim, H., Shin, D., Ji, H.-I., and Lee, J.-H. (2018). A $5 \times 5 \text{ cm}^2$ protonic ceramic fuel cell with a power density of 1.3 W cm^{-2} at 600°C . *Nat. Energy* 3, 870–875.